ELSEVIER

Journal of Chromatography A, 699 (1995) 119–129

JOURNAL OF CHROMATOGRAPHY A

Hollow-fibre flow field-flow fractionation of polystyrene sulphonates

Judith E.G.J. Wijnhoven, Jan Paul Koorn, Hans Poppe, Wim Th. Kok*

Laboratory for Analytical Chemistry, University of Amsterdam, Nieuwe Achtergracht 166, 1018 WV Amsterdam, Netherlands

First received 2 December 1994; revised manuscript received 7 February 1995; accepted 7 February 1995

Abstract

Hollow-fibre flow field-flow fractionation has been used for the characterization and separation of sodium polystyrene sulphonates in aqueous solutions. The elution behaviour of the polymers was found to follow theoretical predictions with a fair accuracy. Diffusion coefficients of standards of different molecular mass could be calculated from elution data. A method was developed to determine the polydispersity of narrow standards by measuring peak widths under different flow regimes. Flow programming has been used to fractionate samples with a wide molecular mass range.

1. Introduction

Field-flow fractionation (FFF), a separation technique which was first developed by Giddings [1], has been shown to be suitable for the separation of a large variety of solutes. The fractionation takes place in an open channel with a laminar flowing liquid. Separation is accomplished by the action of an external field perpendicular to the flow direction. An equilibrium distribution is reached with the molecular diffusion of the molecules or particles (depending on their size) as opposing process. The field distributes different solutes over different streamlines of the parabolic flow profile over the channel width, thereby giving them different velocities in the flow direction (Fig. 1).

A number of subtechniques of FFF can be discerned on basis of the type of field applied, of which three types are the most important in the present state of development. In sedimentation FFF, a gravitational field forces particles to one side of the channel. Separation takes place on basis of differences in density or size of the particles. Sedimentation FFF is mostly used for the separation of (solid) particles with a size ranging from the nm range up to 100 μm [2]. For the fractionation of polymers solved in organic solvents thermal FFF is the most suitable subtechnique [3]. In thermal FFF a temperature gradient is applied across the channel. Depending on their chemical composition and the solvent used, polymer molecules are driven to the cold wall of the channel, a phenomenon known as thermal diffusion. Therefore, in thermal FFF the retention is determined by the ratio of the thermal and molecular diffusion or size of solutes.

Flow FFF, the last developed subtechnique, is the most universal one [4–7]. A second liquid

* Corresponding author.

0021-9673/95/$09.50
SSDI 0021-9673(95)00172-7

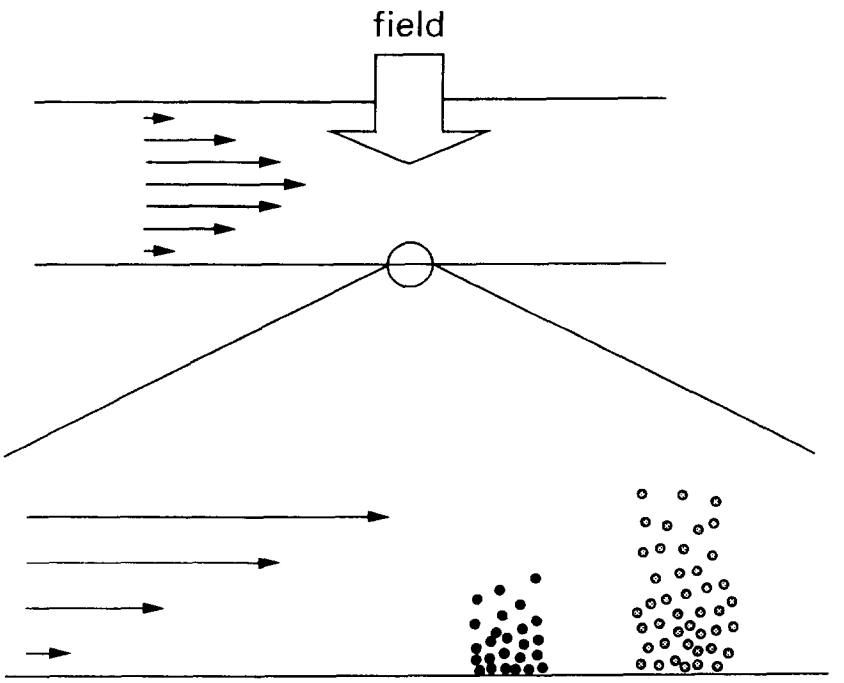

Fig. 1. The FFF separation principle.

flow, perpendicular to the axial flow acts as driving force. This force is the same for all solutes; differentiation in the compression of solutes near the semipermeable wall occurs on basis of differences of the opposing molecular diffusion process. Therefore, retention in flow FFF is solely determined by molecular diffusion, i.e. by the size of the solutes. The applicability of flow FFF is limited by the availability of suitable membrane materials to be used as channel wall. In practice, because of the cut-off characteristics of available membranes, the lower molecular mass limit for solutes is approximately 10 000. Flow FFF is almost exclusively performed with aqueous solvents. The use of organic solvents is still a problem since most membrane materials dissolve in them. Still, a few studies on flow FFF with organic solvents have been published [8,9].

In flow FFF in turn three subtechniques can be discerned, differing in the geometry of the channel and in the way the cross-flow is controlled. The first flow FFF system developed was of the symmetrical type. Here, both walls of a thin, rectangular channel are permeable for the solvent. The cross-flow is delivered through both walls by a second pump in the system, independently of the axial flow (see Fig. 2a). In 1986 an asymmetrical flow FFF system was developed by two different groups [10,11]. In the asymmetrical channel only one of the walls is permeable for the solvent. Originally the other channel wall was made of float glass to make visual inspection of the processes in the channel possible. However, the results obtained with this channel encouraged a further development of the method. In asymmetric flow FFF the cross-flow is a part of the ingoing, axial flow (see Fig. 2b). Asymmetric flow FFF is instrumentally simpler than the symmetric type, since it requires the control of one flow-rate less. Disadvantages are that the axial and cross-flows can not be chosen independently, and that the axial flow is not constant over the length of the channel. In the third type of flow FFF a microporous hollow fibre is used as the separation channel (Fig. 2c). Since the cross-flow is part of the ingoing flow, this variant is of the asymmetric type. In 1974 Lee et al. [12] already conducted studies with a

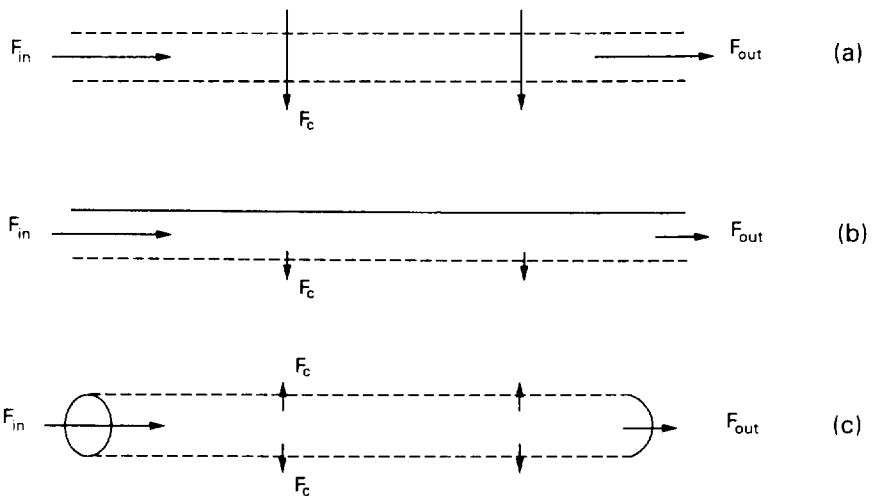

Fig. 2. The three types of flow FFF: symmetrical channel (a), asymmetrical channel (b), and hollow fibre (c).

bundle of hollow fibres, which can be regarded as flow FFF experiments. In 1989 Jönsson and Carlshaf [13] presented their hollow-fibre flow FFF system. The main advantage of their system is its instrumental simplicity; fibres are cheap and easy to install as separation channel. Jönsson and Carlshaf applied the system to the separation of (mostly) polystyrene latex beads studying sample overloading [14], the influence of the ionic strength of the solvent [15] and the properties of various fibre types [16]. Until now, hollow-fibre flow FFF has not been applied for the separation of soluble synthetic polymers. Still, it could be a valuable alternative for size exclusion chromatography (SEC), which is now most often used for the characterization of polymers in solution. In SEC the interaction of the polymers with the packing material may cause problems in the interpretation of the results. In flow FFF interaction can only occur on the fibre wall, which gives a much smaller interaction surface. Moreover, shear degradation, particularly of high-molecular mass polymers, is less likely to occur in flow FFF than in SEC.

In this paper we report on the use of hollow-fibre flow FFF for the characterization and fractionation of sodium polystyrene sulphonates (PSS). Theoretical predictions on the influence of the fibre geometry and the flow regime on the elution behaviour of solved polymers have been verified. The influence of the ionic strength of the solvent on the mass loadability of the system was studied. The possibility to measure the diffusion coefficients of PSS standards in aqueous solutions as a function of the molecular mass has been investigated. Flow programming was used to fractionate a mixture of standards with a wide molecular mass range.

2. Theory

Hollow-fibre flow FFF has been described theoretically by Jönsson and Carlshaf [13], who based their theory on previous work of Lee et al. [4] and Doshi et al. [17]. In the next paragraphs, an approximate theoretical description will be discussed, valid for solutes with moderate to high retention. The basis for this approximative description is the assumption that the solutes are compressed by the cross-flow in a very thin layer with a thickness l near the fibre wall, in a concentration profile given by:

$$c = c_0 \exp\left(-\frac{x}{l}\right) \tag{1}$$

where c_0 is the solute concentration at the fibre wall and x the distance from the wall. In hollow-fibre flow FFF, the layer thickness l for strongly compressed solutes is approximately given by:

$$l = \frac{D}{u_{c,R}} \tag{2}$$

where D is the diffusion coefficient of the solute and $u_{c,R}$ the linear cross-flow velocity through the wall. The axial velocity of the solute in its layer near the wall is then:

$$u_z = \frac{4D}{u_{c,R} \cdot R} \cdot \langle u_z \rangle \tag{3}$$

where R is the inner radius of the fibre and $\langle u_z \rangle$ the mean local flow velocity in the axial direction.

In practical situations the flow resistance of the fibre wall (or membrane) is always much larger than that of the fibre (channel) itself [18]. To obtain the desired cross-flow, the solvent inside the fibre has to be kept at a pressure much higher than the pressure drop over the length of the capillary. Therefore, the cross-flow through the fibre wall is virtually constant over the length of the fibre, and can be written as:

$$u_{c,R} = \frac{F_c}{2\pi RL} \tag{4}$$

where F_c is the total cross-flow rate and L the length of the fibre. The axial flow is then decreasing linearly with the distance from the front end of the fibre, and the mean local axial flow velocity is given by:

$$\langle u_z \rangle = \frac{1}{\pi R^2} \cdot \left(F_{in} - \frac{z}{L} F_c \right) \tag{5}$$

where F_{in} is the total flow-rate entering the fibre and z the distance from the front end of the fibre. Combining Eqs. (3) and (5), the elution time t_r can now be found by integrating $1/u_z$ over the length of the fibre. The result, as given by Jönsson and Carlshaf, is:

$$t_r = \frac{R^2}{8D} \ln \frac{F_{in}}{F_{out}} \tag{6}$$

where F_{out} is the total flow eluting from the end of the fibre ($F_{in} - F_c$).

Doshi et al. [17] also derived expressions for the peak variance in hollow-fibre flow FFF. For strongly retained solutes these can be simplified to:

$$\sigma^2 = \frac{16\pi^2 R^2 L^2 D}{F_c^2} \cdot t_R \tag{7}$$

where σ is the peak standard deviation in time units. In this expression only the non-equilibrium effects are taken into account; the peak broadening by diffusion in the axial direction, which will be small for large polymers, has been neglected.

3. Experimental

3.1. Apparatus

The flow FFF set-up was similar to that used by Jönsson and Carlshaf [13]. In Fig. 3 it is shown schematically. Two P-6000 syringe pumps were controlled by a LCC-500-plus controller (Pharmacia, Uppsala, Sweden). The pump used for the regulation of the cross-flow was con-

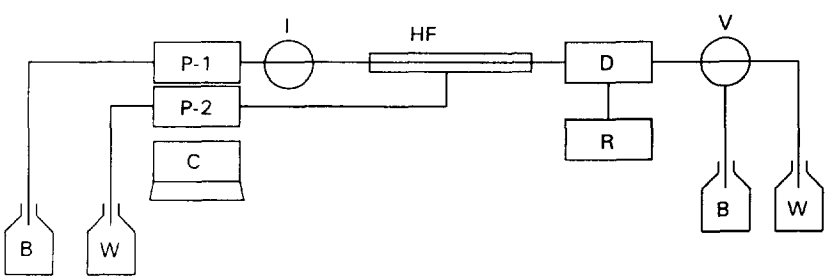

Fig. 3. Experimental set up. (B) Buffer, (W) waste, (P-1) axial flow pump, (P-2) cross-flow pump, (C) controller for pumps, (I) injection valve, (HF) the hollow fibre, (D) detector, (R) recorder or personal computer, (V): switching valve.

nected in such a way that it could suck liquid through the fibre wall. A Rheodyne 7010 injection valve (Rheodyne, Berkeley, CA, USA) with a 5-μl loop was used for sample injection. Detection was performed with a ABI 757 UV absorbance detector (Applied Biosystems, Ramsey, NJ, USA) operated at 235 nm. Signals were registered on a strip-chart recorder. An automated switching valve was inserted in the outlet line of the detector, connecting it to a waste reservoir and a bottle with clean solvent. The PM-100 polysulphon fibres, with a molecular mass cut-off (MWCO) of 100 000, were obtained from Romicon (Woburn, MA, USA). Their length was 20 cm and their inner diameter 1.1 mm (void volume 0.19 ml). The fibres were glued with epoxy glue over poly ether ether keton (PEEK) tubes to connect the fibres with the injector and the detector. The fibre was inserted in a glass tube to which the suction pump for the cross-flow regulation was connected.

3.2. Chemicals and solutions

Sodium polystyrene sulphonate standards, with relative mass average molecular masses of 18 000, 35 000, 100 000, 200 000, 400 000, 780 000 and 1 280 000 were obtained from Polymer Laboratories (Church Stretton, Shropshire, UK). For all standards a polydispersity of less than 1.1 was reported by the supplier. Sample solutions were prepared in demineralized water and stored at 4°C. Solutions of ammonium acetate (p.a. quality) in demineralized water were used as eluent. They were degassed with a helium flow before and during use.

3.3. Procedures

Sample injection and relaxation was performed with an ingoing flow of 0.03 ml/min, the cross-flow was 0.4 ml/min. After injection, it takes some time until the proper concentration profile is formed. This time is considerably longer than the unretained time, t_0. Therefore it is necessary to stop the axial flow to let the concentration profile develop. This is achieved by setting the switching valve at the outlet of the detector in the position that clean solvent was sucked into the outlet of the fibre. After 5 min relaxation period the cross-flow rate was set at the desired value. After 0.2 min, the valve was then switched to the waste reservoir and the ingoing flow-rate was increased to the desired value. All experiments have been performed at least in triplicate, and mean values for elution times and peak widths are reported.

4. Results and discussion

4.1. Retention behaviour

The elution time in hollow-fibre flow FFF is described by Eq. (6). This equation was verified for PSS by varying the experimental parameters. In Fig. 4 the influence of the F_{in}/F_{out} ratio is shown, with F_{in} kept constant at 1.00 ml/min. As expected, the higher M_w standards, having lower diffusion coefficients, are eluted later. The predicted proportionality between t_r and $\ln (F_{in}/F_{out})$ is approximately followed in practice for the different molecular mass standards. The observed deviations from the ideal behaviour may be due to experimental imperfections. For early eluting peaks, the bias of the flow-rates when the pumps are started up after the relaxation procedure, may be relatively important. For late eluting, broad peaks the peak maxima are not always easy to determine accurately.

Eq. (6) also predicts that the elution times are not depending on the length of the fibre used nor on the cross-flow rate, provided that the F_{in}/F_{out} ratio is kept constant. Experiments to verify these predictions have been carried out with 100 000 and 200 000 standards. Fibres of 10 and 20 cm length were used. The cross-flow ranges studied were chosen in such a way that a moderate retention (a retention factor between 0.01 and 0.1) was obtained, to avoid the above mentioned experimental complications as much as possible. The results are shown in Fig. 5. Between the two fibre lengths, no significant differences were found. Although the elution time of highly retained peaks tended to increase

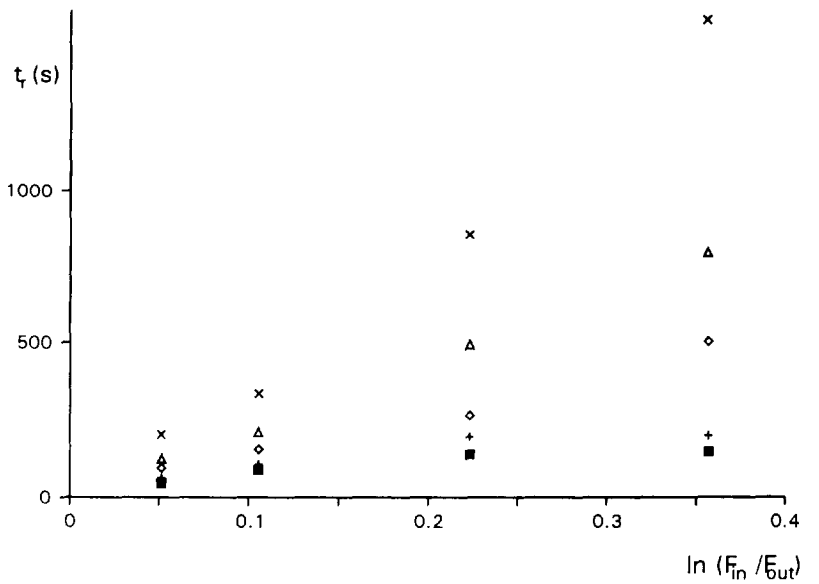

Fig. 4. Influence of the F_{in}/F_{out} ratio on the retention time for five molecular masses. (■) 18 000, (+) 35 000, (◇) 100 000, (△) 200 000, (×) 400 000.

slightly with the cross-flow, the general trend is that the elution time of a PSS standard is independent of the cross-flow. For practical reasons a fibre of 20 cm length was used in the rest of the experiments.

According to theory, the elution time of polymer standards is inversely proportional to their diffusion coefficient. The diffusion coefficient D of polymers can often be expressed by the formula:

$$D = A \cdot M_w^{-b} \tag{8}$$

where M_w is the molecular mass of the polymer and A and b are empirical constants. The constant b is for polymers 0.50 for a poor solvent up

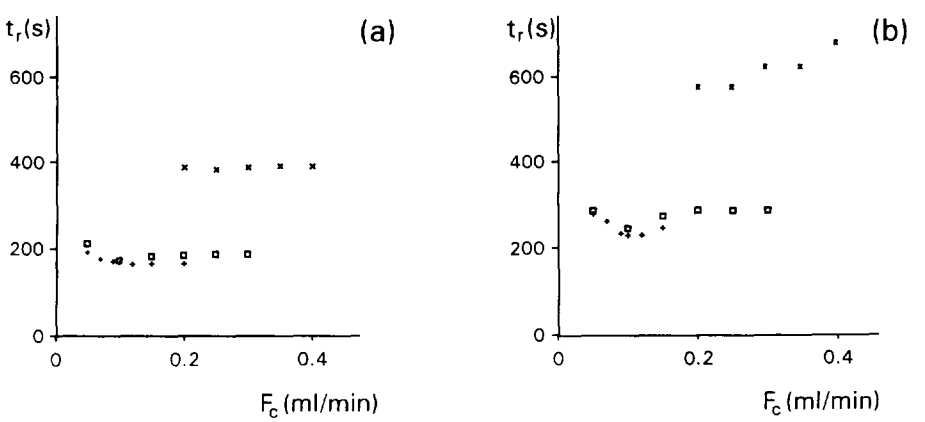

Fig. 5. Retention time as function of the fibre length, (a) molecular mass 100 000, (b) molecular mass 200 000. (+) Fibre length 10 cm, $F_c/F_{in} = 0.1$; (□) fibre length 20 cm, $F_c/F_{in} = 0.1$; (×) fibre length 20 cm, $F_c/F_{in} = 0.2$.

to about 0.59 for a good solvent [19]. Combination of Eqs. (6) and (8) gives the relation between the molecular mass and the elution time in hollow-fibre flow FFF:

$$\log t_r = k + b \cdot \log M_w \quad (9)$$

where k is a constant depending on the flow regime and the type of polymer. In Fig. 6 observed $\log t_r$ values are plotted as a function of $\log M_w$ for various cross-flow rates. Each data point in this figure represents the mean of 6–12 measurements. (The standard deviation of the mean for 4 identical measurements on the same day is 4%. The day-to-day reproducibility is less.) Approximately straight lines are obtained, with slopes b varying from 0.41 for $F_c = 0.10$ ml/min to 0.61 for $F_c = 0.30$ ml/min. In the interpretation of these results it must be realized that the scatter in the individual measurements is relatively large, and that especially the short elution times may be biased by the slow pump start after relaxation. Taking into account only those measurements with reasonably long elution volumes ($V_r > 1.5$ ml), the diffusion coefficients presented in Table 1 were calculated from the data in Fig. 4. With these results Eq. (9) can be written as:

$$D = (1.5 \pm 0.2) \cdot 10^{-8} \cdot M_w^{-0.56 \pm 0.02} (m^2\, s^{-1})$$

The value of b found is close to the theoretical value (0.50–0.59).

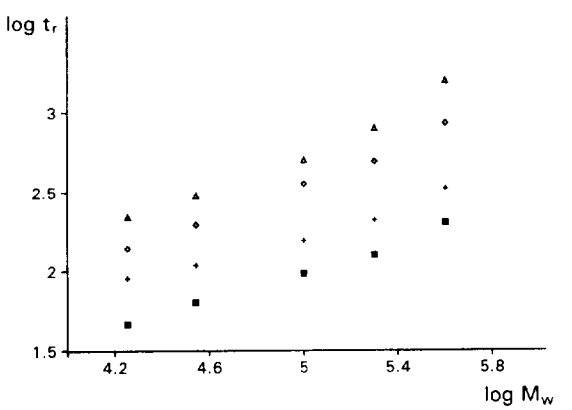

Fig. 6. $\log t - \log M_w$ plots ($F_{in} = 1$ ml/min). (■) $F_c = 0.05$ ml/min, (+) $F_c = 0.1$ ml/min, (◇) $F_c = 0.2$ ml/min, (△) $F_c = 0.3$ ml/min.

Table 1
Calculated diffusion coefficients of PSS standards

M_w	D (10^{-11} m^2 s^{-1})[a]	-log D[a]
18 000	5.8 ± 0.6	6.23 ± 0.04
35 000	4.1 ± 0.5	6.39 ± 0.05
100 000	2.6 ± 0.3	6.59 ± 0.06
200 000	1.7 ± 0.2	6.77 ± 0.06
400 000	1.0 ± 0.2	6.99 ± 0.08

[a] Mean ± standard deviation in the single measurements.

Literature data on diffusion coefficients of PSS in the size range as used here, are scarce. Kirkland et al. [20] reports values which agree with our results, although the ionic strengths of the eluents are different from ours. Koene and Mandel [21] reports a value of $0.91 \cdot 10^{-11}$ m^2 s^{-1} for a 400 000 standard at low concentration (0.01 g/l) in 0.01 mol/l NaCl solution, as measured by quasi-elastic light scattering. This agrees well with our result ($1.04 \pm 0.21 \cdot 10^{-11}$ m^2 s^{-2}). Koene found that the diffusion coefficient increased with the concentration of the polymer in the solution. Although the polymer concentration in the eluate in our experiments was low, with typically 0.5 μg of the polymer per injection eluted in a peak volume of 1–3 ml, during the separation the polymer is strongly concentrated near the fibre wall. Therefore, the apparent diffusion coefficient found with hollow-fibre flow FFF can be expected to be higher than the value for infinite dilution.

This aspect was further studied by measuring the elution times with the injection of a 100 000 standard in various concentrations. Two elution solvents were used, containing 0.0001 and 0.01 mol/l ammonium acetate, respectively. In Fig. 7 $1/t_r$ is plotted as a function of the amount of solute injected. With the low-ionic strength solvent, $1/t_r$ increases approximately linear with the injected amount. This could be the result of a linear increase of the diffusion coefficient with the concentration, as was also found by light scattering measurements [21]. With the 0.01 mol/l ionic strength solvent the effect of the solute concentration on the elution time was not found. Therefore, the mutual electrostatic repulsion of

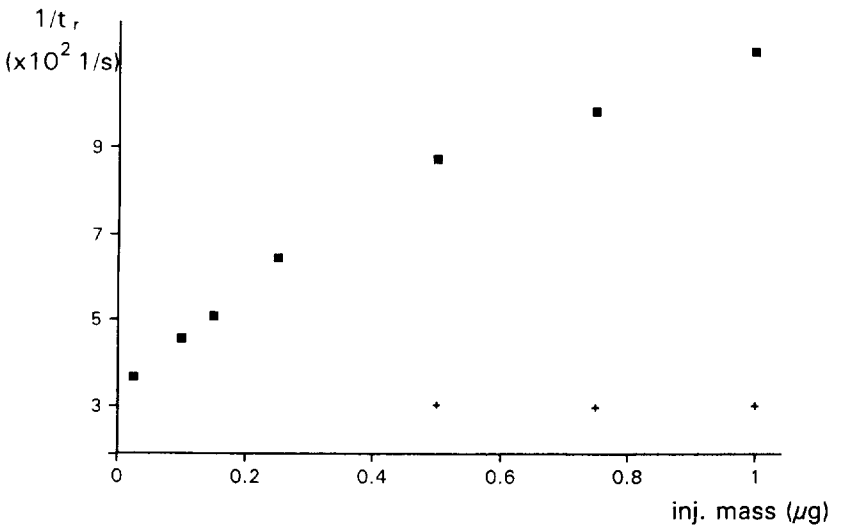

Fig. 7. Influence of the injected mass on the reciprocal of the retention time for two different ionic strengths. (+) Ionic strength = 0.01 mol/l, (■) ionic strength 0.0001 mol/l.

the charged polymers may be a more translucent explanation for their behaviour in a low-ionic strength solution. Such a repulsion would set a limit to the compression of the solute near the fibre wall. As a result, the solute layer thickness, and with that the average axial velocity of the solute, increases with the amount injected. Electrostatic repulsion can also be regarded as the underlying principle of the increase of the apparent diffusion coefficients obtained from light scattering experiments. Since extrapolation of the experimental data to $c_{inj} = 0$ gives approximately similar elution times for infinitely diluted samples in different ionic strength solvents, electrostatic repulsion by the fibre probably does not play a major role.

4.2. Measurement of polydispersities

The width of peaks in hollow fibre flow FFF is determined by the system peak broadening, as described in Eq. (7), and by the polydispersity μ (defined as M_w/M_n) of the polymer sample injected. Since μ can be expressed as [22]:

$$\mu = 1 + \frac{\sigma_M^2}{M_w^2} \tag{11}$$

where σ_M is the standard deviation of the molecular mass distribution in mass units, it can easily be shown that the polydispersity causes a peak variance in the fractionation system given by:

$$\sigma_p^2 = b^2(\mu - 1)t_r^2 \tag{12}$$

where σ_p is in time units and t_r is the elution time of the number average molecular mass (M_n) of the sample.

A problem in the determination of polydispersities is the discrimination between the system and the sample contributions to σ^2, since for the calibration of the system a sample with a finite polydispersity has to be used. However, by combination of Eqs. (6), (7) and (12) the total peak variance can be described by:

$$\frac{\sigma_{tot}^2}{t_r^2} = \frac{128\pi^2 L^2 D^2}{F_c^2 \ln(F_{in}/F_{out})} + b^2(\mu - 1) \tag{13}$$

Peak variances and retention times have been measured for polymer standards under different flow regimes. In Fig. 8 σ^2/t_r^2 values (the reciprocal of the obtained plate number) have been plotted as a function of $1/(F_c^2 \ln (F_{in}/F_{out}))$ for the 100 000, 200 000, and 400 000 standards. For the retention times the mean values over a series of experiments with equal F_{in}/F_{out} ratio were

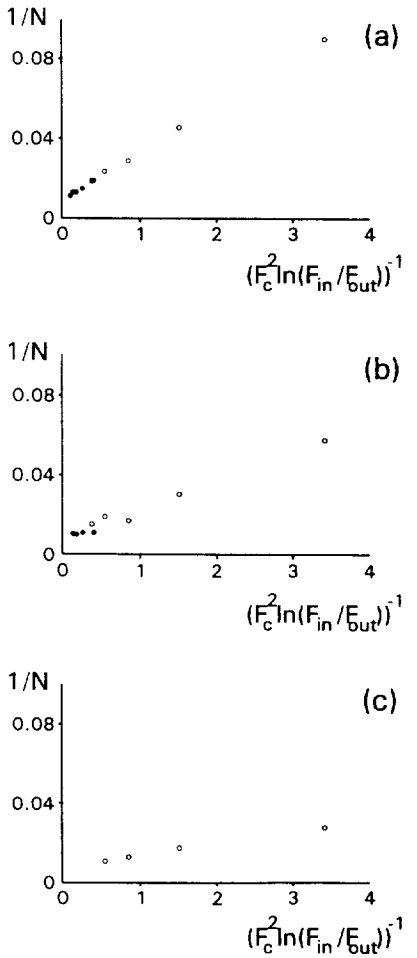

Fig. 8. Plot of the reciprocal of the plate number as a function of $(F_c^2/\ln(F_{in}/F_{out}))^{-1}$. (a) Molecular mass 100 000, (b) molecular mass 200 000, (c) molecular mass 400 000. (○) $F_c - F_{in} = 0.1$, (●) $F_c - F_{in} = 0.2$.

used. According to Eq. (13), straight lines should be obtained with a slope depending on the diffusion coefficient of the standard. As can be seen in the figure, the experimental data follow this prediction with a fair accuracy. Intercepts and slopes of the plots were calculated by linear regression. From these, values for μ were calculated as given in Table 2, using a value of 0.56 for b. The polydispersities of the samples appeared to be considerably smaller than had been indicated by the supplier (less than 1.1 for all standards). The stated ceiling values for the polydispersity appear to be conservative estimates, a fact also mentioned by other authors [23,24].

Table 2
Measurement of the polydispersities of the PSS standards

M_w	Intercept in Fig. 8[a]	μ
100 000	0.0092 ± 0.0007	1.029 ± 0.002
200 000	0.0079 ± 0.0021	1.025 ± 0.007
400 000	0.0077 ± 0.0006	1.024 ± 0.002

[a] Standard deviations of the mean.

From the slopes of the plots D can be obtained. For the 100 000, 200 000 and 400 000 standards values of 2.2, 1.7 and $1.1 \cdot 10^{-11}$ $m^2 s^{-1}$ were found, respectively. These values are in fair agreement with those obtained directly from their elution time (Table 1), which indicates that the proposed method to determine the polydispersity is reliable.

4.3. Application as fractionation method

In the first stage of our experiments PSS standards with molecular masses of 780 000 and 1 280 000 were included in the test set. However, with these standards irregular and irreproducible results were obtained. In light scattering experiments it has been shown previously that PSS molecules with these high molecular masses are very sensitive to degradation in solution [25]. Therefore, in further experiments these standards were not used. The low M_w standards (18 000 and 35 000) were not always completely recovered from the fibre, especially with high cross-flows and high-ionic strength solutions. Apparently, these polymers were not excluded sufficiently from the fibre pores under these conditions. A separation of the 18 000 and 35 000 standards was not possible; to obtain sufficient separation from the void volume peak, an initial cross-flow rate had to be used at which the fibre becomes permeable for the smallest polymers.

The reproducibility of the elution times of standards was in the order of 5% when a series of consecutive measurements was carried out. However, the day-to-day reproducibility was by

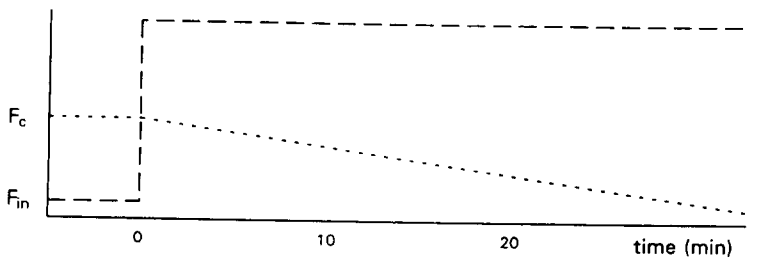

Fig. 9. Flow program for gradient elution. F_{in} is set at 0.05 ml/min, F_c at 0.45 ml/min, one minute later the sample is injected and the relaxation phase starts. After 5 min F_{in} is set to its elution value (1 ml/min), from that point the cross-flow diminishes (with 0.01 ml/min) linear to 0 ml/min.

far inferior, and when a different fibre had been installed the elution times could change by 10%. Similar findings have been reported by Carlshaf and Jönsson, who tested fibres from different sources [16]. It is clear that a first requirement for a wider application of hollow-fibre flow FFF is the availability of more reproducible and stable fibres.

For the separation of a wide range of standards (from 35 000 to 400 000) a flow gradient was used. A simple linear flow programme was used as shown in Fig. 9. The 18 000 standard was not recovered under these conditions: cross-flow rates were too high. For the other standards a baseline separation was obtained in 30 min (see Fig. 10). The main peak broadening contribution under the conditions applied is the polydispersity of the standards.

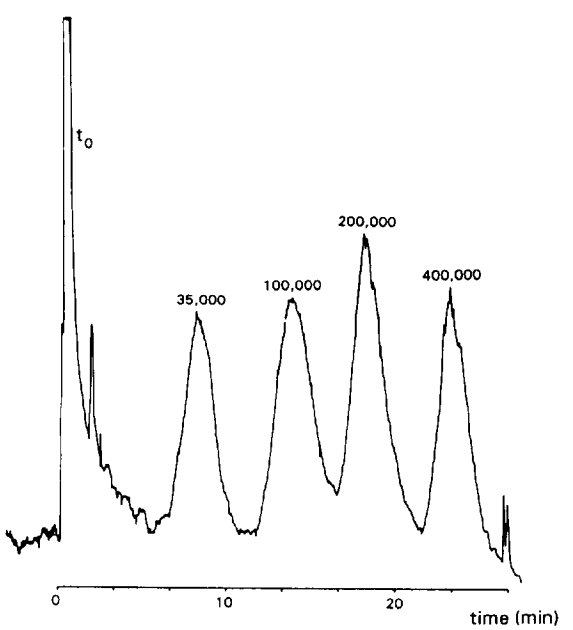

Fig. 10. Separation of PSS standards, F_{in} 1.0 ml/min, F_c 0.4 ml/min in 45 min, ionic strength 0.01 mol/l.

References

[1] J.C. Giddings, *Sep. Sci.*, 1 (1966) 123.
[2] J.C. Giddings, F.J.F. Yang and M.N. Myers, *Anal. Chem.*, 46 (1974) 1917.
[3] M.E. Schimpf, *J. Chromatogr.*, 517 (1990) 405.
[4] H.L. Lee and E.N. Lightfoot, *Sep. Sci.*, 11 (1976) 417.
[5] J.C. Giddings, F.J.F. Yang and M.N. Myers, *Science*, 193 (1976) 1244.
[6] J.C. Giddings, F.J.F. Yang and M.N. Myers, *Anal. Chem.*, 48 (1976) 1126.
[7] S.K. Ratanatanawongs and J.C. Giddings, *ACS Symp. Ser.*, 521 (1993) 13.
[8] S.L. Brimhall, M.N. Myers, K.D. Caldwell and J.C. Giddings, *J. Pol. Sci. Pol. Lett. Ed.*, 22 (1984) 339.
[9] J.J. Kirkland and C.H. Dilks Jr., *Anal. Chem.*, 64 (1992) 2836.
[10] J. Granger, J. Dodds, D. Leclerc and N. Midoux, *Chem. Eng. Sci.*, 41 (1986) 3119.
[11] K.G. Wahlund and J.C. Giddings, *Anal. Chem.*, 59 (1987) 1332.
[12] H.L. Lee, J.F.G. Reis, J. Dohner and E.N. Lightfoot, *AICHE J.*, 20 (1974) 776.
[13] J.Å. Jönsson and A. Carlshaf, *Anal. Chem.*, 61 (1989) 11.
[14] A. Carlshaf and J.Å. Jönsson, *Sep. Sci. Tech.*, 28 (1993) 1191.
[15] A. Carlshaf and J.Å. Jönsson, *J. Microcol. Sep.*, 3 (1991) 411.
[16] A. Carlshaf and J.Å. Jönsson, *Sep. Sci. Technol.*, 28 (1993) 1031.
[17] M.R. Doshi, W.N. Gill and R.S. Subramanian, *Chem. Eng. Sci.*, 30 (1975) 1467.

[18] A. Litzén, *Anal. Chem.*, 65 (1993) 461.
[19] C. Tanford, *Physical Chemistry of Macromolecules*, Wiley and sons, New York–London, 1961.
[20] J.J. Kirkland, C.H. Dilks and S.W. Rementer, *Anal. Chem.*, 64 (1992) 1295.
[21] R.S. Koene and M. Mandel, *Macromolecules*, 16 (1983) 220.
[22] J.H. Knox and F. McLennan, *Chromatographia*, 10 (1977) 75.
[23] M.F. Schimpf, M.N. Myers and J.C. Giddings, *J. Appl. Polym. Sci.*, 33 (1987) 117.
[24] G. Stegeman, J.C. Kraak and H. Poppe, *J. Chromatogr.*, 634 (1993) 149.
[25] J. van Dijk, Department of Physical and Macromolecular Chemistry, University of Leiden, personal communication.